

# *The tropopause inversion layer in models and analyses*

Article

Published Version

Birner, T., Sankey, D. and Shepherd, T. G. (2006) The tropopause inversion layer in models and analyses. *Geophysical Research Letters*, 33 (14). L14804. ISSN 0094-8276 doi: <https://doi.org/10.1029/2006GL026549> Available at <https://centaur.reading.ac.uk/32067/>

It is advisable to refer to the publisher's version if you intend to cite from the work. See [Guidance on citing](#).

Published version at: <http://dx.doi.org/10.1029/2006GL026549>

To link to this article DOI: <http://dx.doi.org/10.1029/2006GL026549>

Publisher: American Geophysical Union

All outputs in CentAUR are protected by Intellectual Property Rights law, including copyright law. Copyright and IPR is retained by the creators or other copyright holders. Terms and conditions for use of this material are defined in the [End User Agreement](#).

[www.reading.ac.uk/centaur](http://www.reading.ac.uk/centaur)

**CentAUR**

Central Archive at the University of Reading

Reading's research outputs online

# The tropopause inversion layer in models and analyses

T. Birner,<sup>1</sup> D. Sankey,<sup>1</sup> and T. G. Shepherd<sup>1</sup>

Received 10 April 2006; revised 19 May 2006; accepted 13 June 2006; published 19 July 2006.

[1] Recent high-resolution radiosonde climatologies have revealed a tropopause inversion layer (TIL) in the extratropics: temperature strongly increases just above a sharp local cold point tropopause. Here, it is asked to what extent a TIL exists in current general circulation models (GCMs) and meteorological analyses. Only a weak hint of a TIL exists in NCEP/NCAR reanalysis data. In contrast, the Canadian Middle Atmosphere Model (CMAM), a comprehensive GCM, exhibits a TIL of realistic strength. However, in data assimilation mode CMAM exhibits a much weaker TIL, especially in the Southern Hemisphere where only coarse satellite data are available. The discrepancy between the analyses and the GCM is thus hypothesized to be mainly due to data assimilation acting to smooth the observed strong curvature in temperature around the tropopause. This is confirmed in the reanalysis where the stratification around the tropopause exhibits a strong discontinuity at the start of the satellite era. **Citation:** Birner, T., D. Sankey, and T. G. Shepherd (2006), The tropopause inversion layer in models and analyses, *Geophys. Res. Lett.*, 33, L14804, doi:10.1029/2006GL026549.

## 1. Introduction

[2] The tropopause is an important climate feature and, e.g., has recently been suggested to be a useful indicator of climate change [Santer *et al.*, 2003]. The sharp vertical change in thermal stratification at the tropopause has implications for the distribution of trace gases such as ozone and water vapor. A detailed understanding of the thermal stratification around the tropopause is therefore crucial for an understanding of the tropopause itself, the climate system and climate change.

[3] Recent high-resolution radiosonde (HRRS for short hereafter) climatologies of the thermal structure of the extratropical tropopause region have revealed the existence of a tropopause inversion layer (TIL) [Birner *et al.*, 2002; Birner, 2006]: the vertical temperature gradient exhibits a strong inversion at the extratropical tropopause, i.e., temperature strongly increases just above a sharp local cold point tropopause. Correspondingly, buoyancy frequency squared ( $N^2$ ) maximizes within this TIL, i.e., values of  $N^2$  are considerably enhanced compared to stratospheric values of  $N^2$  further aloft. The method of averaging (see next section) was crucial to uncover the TIL. The TIL was shown to climatologically exist above Southern Germany [Birner *et al.*, 2002] and North America [Birner, 2006]. Although the cause of the TIL has yet to be understood, its character-

istics must have implications for dynamics and tracer transport in this region of the atmosphere. The present study addresses the question to what extent a TIL exists in meteorological analyses and/or current GCMs. Data from the NCEP/NCAR reanalysis (NCEP-RA for short hereafter) and the Canadian Middle Atmosphere Model (CMAM), in both free-running and data assimilation (DA) mode, are evaluated. Emphasis is placed on the impact of DA on the representation of the thermal structure around the extratropical tropopause.

## 2. Data Sets and Methodology

[4] CMAM constitutes a comprehensive GCM with interactive chemistry. Dynamics and chemical transport are calculated using a T47 spectral representation. Vertically the model has 71 layers, extending to around 100 km altitude. Around the extratropical tropopause the vertical resolution  $\Delta z_{\text{CMAM}} \sim 0.9\text{--}1.2$  km. A much more detailed description of an earlier version of the model is given by Beagley *et al.* [1997]. In the case of the free-running version (hereafter referred to as CMAM) output from two months (January and July) taken from the second year of integration (arbitrary) is analyzed. The data assimilation version (CMAM-DA) uses 3D-Var assimilation and is described by Polavarapu *et al.* [2005]. Output from January and July 2002 is analyzed for CMAM-DA.

[5] The NCEP-RA data are described by Kalnay *et al.* [1996]. Dynamics are calculated using a T63 spectral grid on 28 vertical levels. It is important in the present context to use data on model levels, since data on standard pressure levels (as conventionally used) do not contain sufficient vertical information close to the tropopause. Around the extratropical tropopause the vertical resolution  $\Delta z_{\text{NCEP-RA}} \sim 1.2\text{--}1.5$  km.

[6] In order to derive climatologies of the thermal structure around the tropopause, temperature is first transformed from spectral space to a regular lat-lon grid. Averages are then computed by employing the tropopause-based (TB) method described by Birner *et al.* [2002] and Birner [2006]. This method utilizes the tropopause itself as a common reference level for all vertical profiles within the mean, i.e., profiles are averaged with respect to the local, time-dependent tropopause level. Conventional averages would blur sharp features coupled to the tropopause, whereas they are preserved in a TB-mean. It is desirable to use a vertical coordinate that yields about constant vertical resolution when computing the TB-mean in order to ensure equal representation of profiles with different tropopause levels. The HRRS data has about constant resolution in  $z$ . Therefore,  $z - z_{\text{TP}}$  (subscript TP denotes tropopause hereafter) was used as vertical coordinate for the TB-mean in the case of the HRRS. However, in the case of the NCEP-RA model and CMAM the vertical resolution is variable in  $z$  but about

<sup>1</sup>Department of Physics, University of Toronto, Toronto, Ontario, Canada.

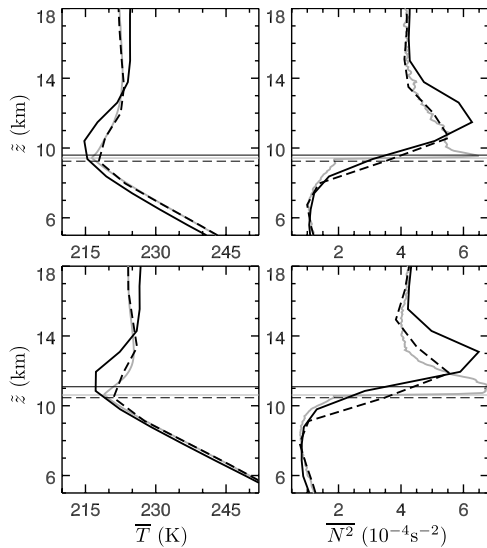


**Figure 1.** (left) TB-mean profiles of temperature and (right) buoyancy frequency squared over Alaska around  $60^\circ$  N, for CMAM (full), NCEP-RA (dashed, 1998–2002), HRRS (gray, 1998–2002). TB-mean for HRRS has been computed in  $z - z_{TP}$  but is plotted in log-pressure altitude  $\tilde{z}$ . (top) January, (bottom) July. Horizontal lines denote  $\tilde{z}_{TP}$ .

constant in  $\Pi = T/\Theta$ , a pressure-like coordinate, with  $T$  - temperature and  $\Theta$  - potential temperature. Therefore  $\Pi - \Pi_{TP}$  is used as vertical coordinate for the TB-mean in the present study. An algorithm similar to that described by Reichler *et al.* [2003] is used to determine  $\Pi_{TP}$ . For plotting purposes fields are re-shifted with respect to the mean tropopause level and transformed to log-pressure altitudes, denoted by  $\tilde{z}$ .

### 3. Results

[7] Figure 1 compares the TB-mean thermal structure representative of Alaska around  $60^\circ$  N, from CMAM and the NCEP-RA to the HRRS. Only those geographical locations of all U.S. radiosonde stations within [ $55^\circ$  N,  $65^\circ$  N] are used (see Birner [2006] for a description of the HRRS data set). Both CMAM and NCEP-RA fields were interpolated onto the station locations prior to computing the TB-mean.

[8] The TB-mean profiles from HRRS around  $60^\circ$  N exhibit a clear TIL (strongly increasing temperature just above a sharp local cold point tropopause, correspondingly a local maximum in  $N^2$ ) in both winter and summer. As discussed by Birner [2006] there exists a distinct winter-summer contrast in that maximum values of  $N^2$  are larger in summer and concentrated in a thinner layer compared to winter. TB-mean profiles from NCEP-RA only exhibit a weak hint of a TIL, seemingly due to the much coarser vertical resolution in this data set ( $\Delta z_{NCEP-RA} : \Delta z_{HRRS} \sim 50 : 1$ ). The NCEP-RA profiles roughly sample the HRRS profiles at their resolution. No winter-summer contrast is evident in the NCEP-RA profiles. TB-mean profiles from CMAM, in contrast to NCEP-RA, exhibit a distinct TIL, even though CMAM has comparable resolution to NCEP-RA. CMAM profiles also show a realistic winter-

summer contrast. However, the TIL in CMAM is located distinctly higher above the tropopause than in the observations (HRRS), i.e., the cold layer around the local tropopause is too deep. Note that there are small biases in temperature in CMAM compared to the HRRS that may in part be due to the fact that only one arbitrary January/July from CMAM is compared to the HRRS climatology. However, the qualitative vertical structure is not affected by these biases.

[9] Figure 2 shows TB zonal mean, time mean latitude-height cross sections of the thermal structure of the global tropopause region in CMAM, CMAM-DA, and NCEP-RA (a similar cross section for the HRRS over the U.S. is contained in Figure 7 of Birner [2006]). As is the case for Alaska, NCEP-RA only exhibits a weak hint of a TIL (values of  $N^2$  are only slightly enhanced just above the tropopause). The weak maximum in  $N^2$  just above the extratropical tropopause does not show a winter-summer contrast in the northern hemisphere (NH). In the southern hemisphere (SH) a very weak TIL more or less similar to the one in the NH exists in winter (July) whereas in summer (January) no distinct structure exists. A similar picture emerges from the European Centre for Medium-Range Weather Forecasts Reanalysis (ERA40) data (not shown).

[10] In contrast, CMAM shows a very distinct TIL in both hemispheres with a marked winter-summer contrast. The TIL in CMAM appears qualitatively symmetric around the equator when comparing the same season. In the case of CMAM-DA the TIL becomes much less distinct, especially in the SH summer. No strong winter-summer contrast is evident anymore. Apparently, the data assimilation procedure in CMAM-DA leads to a strongly weakened TIL that does not agree well with observations. Note that CMAM-DA shows weakened values of  $N^2$  compared to CMAM just above the tropical tropopause as well, although a detailed investigation of this feature is beyond the scope of the present study. Data assimilation seems to generally act to smooth sharp structures such as those tied to the tropopause. This seems to be most prominent in the SH where only satellite data with coarse vertical resolution is available.

[11] In order to test our hypothesis that DA smoothes the thermal structure close to the tropopause, the following sensitivities are investigated. DA was operationally incorporated into CMAM starting 15 December 2001, 00 UT. This represents a ‘switch on’ sensitivity experiment which can be used to study the temporal evolution of the maximum value of  $N^2$  ( $N_{max}^2$ ) just above the tropopause after DA is ‘switched on’. Figure 3 shows the temporal evolution of  $N_{max}^2$  obtained from instantaneous zonal TB-mean profiles, averaged globally and over northern and southern midlatitudes (here defined as  $45^\circ$ – $75^\circ$ ). When DA is switched on  $N_{max}^2$  drops by about 10% (NH) and by almost 20% (SH) within about 3 (NH) and 5 (SH) days, respectively. On the global scale  $N_{max}^2$  drops by about 5% within one day. It is interesting to note that  $N_{max}^2$  settles on about the same value in the SH and NH, even though initially it was much larger in the SH (due to the winter-summer contrast).

[12] What happens if DA is switched off again? Figure 3 further shows the temporal evolution of  $N_{max}^2$  over one month after DA was switched off (January 2002). After a few days  $N_{max}^2$  starts adjusting back to its free-running background value. The time-scale for this re-adjustment can be inferred to be on the order of 3 weeks.



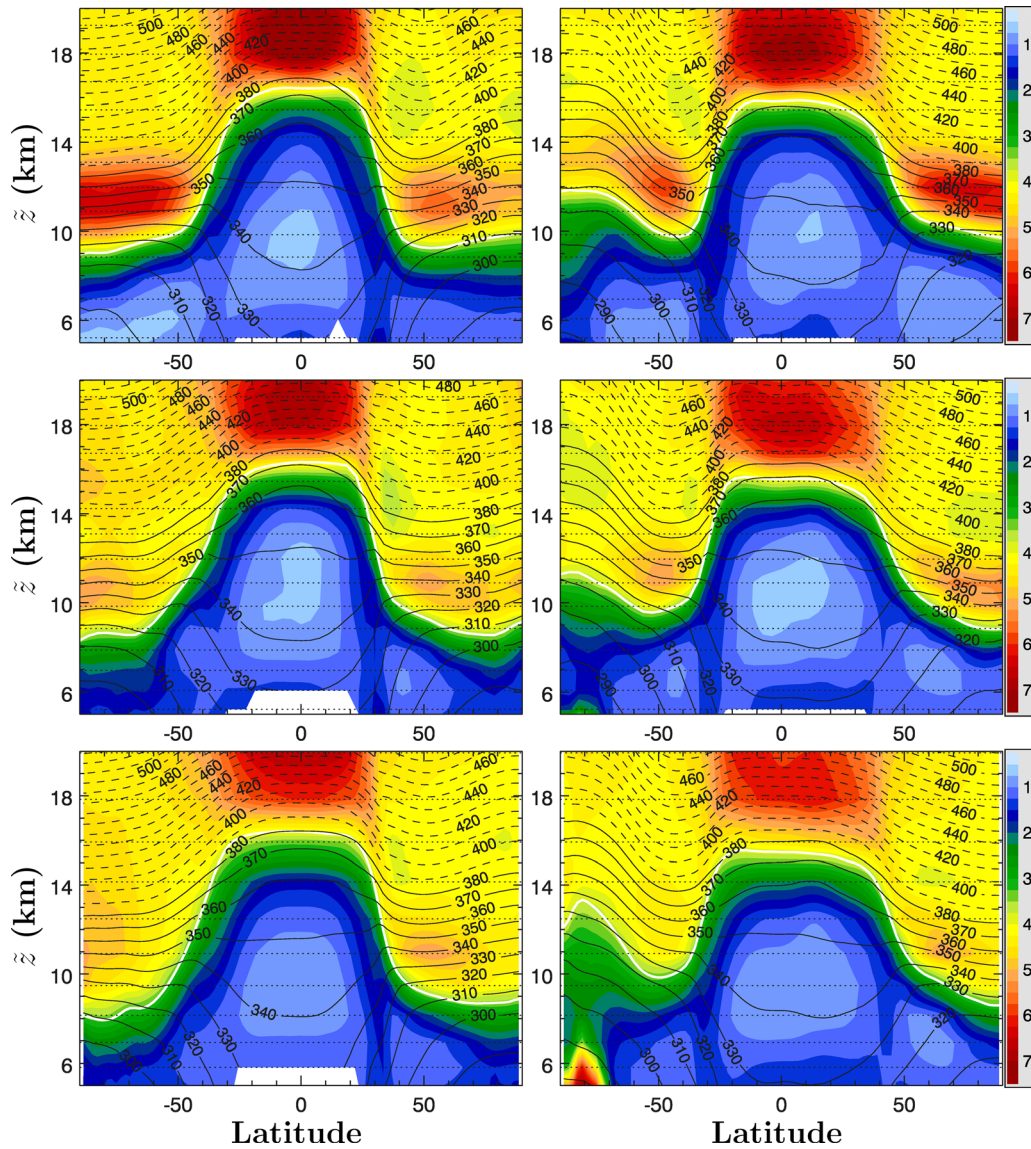


**Figure 2.** Zonal mean TB-mean buoyancy frequency squared ( $10^{-4} \text{ s}^{-2}$ , color shading) and isentropes (contours, overworld dashed). (left) January, (right) July. From top to bottom: CMAM, CMAM-DA (year 2002), NCEP-RA (years 1998–2002). Thick white lines denote  $\bar{z}_{\text{TP}}$ . Dotted horizontal lines mark approximate location of model levels.

[13] We cannot perform the same sensitivity tests with the NCEP-RA. However, there are ‘natural’ sensitivity tests included within the RA system. Assimilation of satellite data (the main data contributor in the SH), started mainly in 1979, whereas assimilation of radiosonde data (mainly in the NH) started in the early sixties. It is therefore useful to analyze  $N_{\text{max}}^2$  over the full available NCEP-RA period (1948–2005). Figure 4 (top) shows time-series of  $N_{\text{max}}^2$  from 1948–2005 obtained in the same way as for CMAM, but averaged over consecutive years. A distinct jump in  $N_{\text{max}}^2$  toward smaller values exists in the SH when satellite data start to be assimilated (1979). No such jump is evident in the NH in 1979. However, in the NH,  $N_{\text{max}}^2$  seems to undergo a jump-like behavior toward larger values in the early sixties when radiosonde data start to be assimilated. Globally, the jump in  $N_{\text{max}}^2$  is still very evident, as is the case in the tropics (not shown).

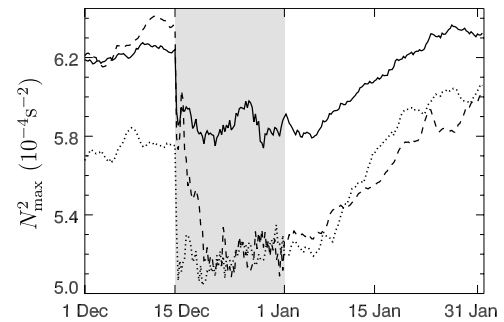


**Figure 3.** Time-series of  $N_{\text{max}}^2$  from CMAM (see text) for December 2001–January 2002. DA is switched on 15 December, 00 UT and switched off 1 January, 00 UT (indicated by gray shading). Global mean (full),  $45^\circ \text{ S}–75^\circ \text{ S}$  (dashed),  $45^\circ \text{ N}–75^\circ \text{ N}$  (dotted).

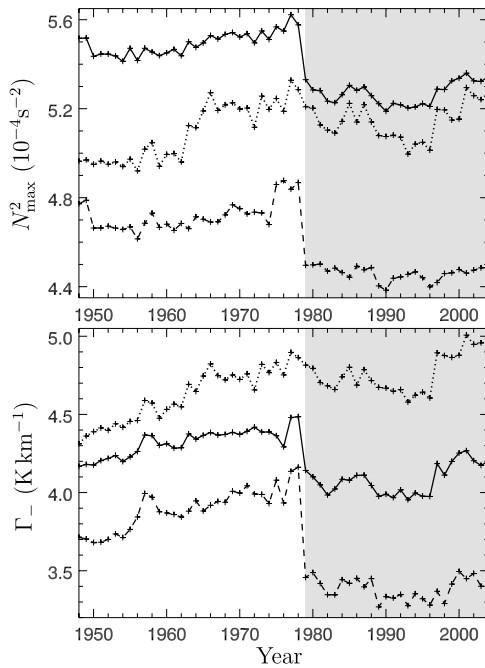


**Figure 4.** Time-series of yearly averaged  $N_{\max}^2$  (top) and  $\Gamma_-$  (bottom) from NCEP-RA. The satellite era started in 1979 (indicated by gray shading). Global mean (full), 45° S–75° S (dashed), 45° N–75° N (dotted).

[14]  $N_{\max}^2$  is a measure of the thermal stratification just above the tropopause, i.e., of the lowermost stratosphere. However, DA will smooth the curvature of the vertical temperature structure around the tropopause. Therefore, the thermal stratification just below the tropopause should be affected by the DA procedure in a similar way to  $N_{\max}^2$ . Figure 4 (bottom) shows time-series of the lapse rate one level below the tropopause ( $\Gamma_-$ ), i.e., roughly 1 km below the tropopause, averaged yearly and over the same latitude bands as in the case of  $N_{\max}^2$ . A distinct jump in  $\Gamma_-$  toward smaller values (larger stratification) exists in the SH in 1979 when satellite data start to be assimilated. In the NH only a weak transition toward larger  $\Gamma_-$  (smaller stratification) in the early sixties exists when radiosonde data start to be assimilated. However, there seems to be a jump in 1997 in the NH. It is interesting to note that the apparent (positive) trend in  $\Gamma_-$  in the NH between about 1965 and 1978 (pre-satellite) seems to be continued after 1997, although more data after 2005 is needed to confirm this. Note also that the satellite data seem to induce a trend inversion in the NH until 1997. Finally it is noted that the hemispheric difference in the behavior at 1979 is more pronounced in the case of  $\Gamma_-$  than in the case of  $N_{\max}^2$ .

#### 4. Conclusions

[15] High-resolution radiosonde observations show a layer with distinct thermal properties that lies just above the extratropical tropopause - the tropopause inversion layer (TIL) [Birner et al., 2002; Birner, 2006]. The present study shows that such a layer exists in CMAM, a middle atmosphere GCM. It exhibits a realistic winter-summer contrast

and exists in both the NH and SH. In contrast, state-of-the-art reanalysis data exhibit only a weak hint of a TIL. Since CMAM and the NCEP-RA have similar vertical resolution close to the tropopause, vertical resolution is apparently not the issue. It is hypothesized that the weakened TIL in the NCEP-RA is due to data assimilation (DA) acting to smooth the sharp vertical temperature structure around the tropopause underlying the TIL. In fact, CMAM-DA - a version of CMAM that includes DA - exhibits a strongly weakened TIL that rather resembles the one found in the NCEP-RA. Time-series analysis of  $N_{\max}^2$  (a quantity describing the strength of the TIL) shows that the TIL almost disappears after the first few days once DA is switched on in CMAM; whereas it takes on the order of 3 weeks to re-establish CMAM's TIL once DA is switched off again. The impact of DA on the thermal stratification just above the tropopause (i.e., to what extent a TIL exists) is strongest in regions where satellite data are the major contributor to the DA procedure (i.e. in the SH). In the case of the NCEP-RA the impact of (vertically coarse) satellite data on the vertical temperature structure around the tropopause becomes strongly evident in the behavior of time-series of  $N_{\max}^2$  and  $\Gamma_-$  in 1979 when satellite data start to be assimilated.

[16] The present results have shown that DA acts to smooth sharp structures in key meteorological quantities such as temperature. This smoothing is due in part to the error covariances, and in part to coarse input data such as nadir satellite measurements (as seen in the difference between the NH and SH). Future meteorological analyses will have to take this effect into account if they are to reproduce a realistic thermal structure around the tropopause. The wind structure can be assumed to be affected in a similar way through thermal wind balance.

[17] **Acknowledgments.** This work has been supported by Environment Canada, the Natural Sciences and Engineering Research Council, the Canadian Foundation for Climate and Atmospheric Sciences, and the Canadian Space Agency. NCEP-RA data were provided by the NOAA-CIRES Climate Diagnostics Center (<http://www.cdc.noaa.gov/>). The U.S. radiosonde data are freely available at the SPARC data center (<http://www.sparc.sunysb.edu/>). Helpful comments were provided by two anonymous reviewers.

#### References

- Beagley, S. R., J. de Grandpré, J. Koshyk, N. A. McFarlane, and T. G. Shepherd (1997), Radiative-dynamical climatology of the first-generation Canadian Middle Atmosphere Model, *Atmos. Ocean*, 35, 293–331.
- Birner, T. (2006), Fine-scale structure of the extratropical tropopause region, *J. Geophys. Res.*, 111, D04104, doi:10.1029/2005JD006301.
- Birner, T., A. Dörnbrack, and U. Schumann (2002), How sharp is the tropopause at midlatitudes?, *Geophys. Res. Lett.*, 29(14), 1700, doi:10.1029/2002GL015142.
- Kalnay, E., et al. (1996), The NCEP/NCAR 40-year reanalysis project, *Bull. Am. Meteorol. Soc.*, 77, 437–471.
- Polavarapu, S., S. Z. Ren, Y. Rochon, D. Sankey, N. Ek, J. Koshyk, and D. Tarasick (2005), Data assimilation with the Canadian middle atmosphere model, *Atmos. Ocean*, 43, 77–100.
- Reichler, T., M. Dameris, and R. Sausen (2003), Determining the tropopause height from gridded data, *Geophys. Res. Lett.*, 30(20), 2042, doi:10.1029/2003GL018240.
- Santer, B. D., et al. (2003), Contributions of anthropogenic and natural forcing to recent tropopause height changes, *Science*, 301, 479–483.

T. Birner, D. Sankey, and T. G. Shepherd, Department of Physics, University of Toronto, 60 St George Street, Toronto, ON, Canada M5S 1A7. (thomas@atmosph.physics.utoronto.ca)